Structural Decomposition Approach for Distribution Network Reconfiguration

Chenchen Li, *Graduate Student Member, IEEE*, Nian Liu, *Member, IEEE*, Liudong Chen, *Graduate Student Member, IEEE*, Yubing Chen, and João P. S. Catalão, *Fellow, IEEE*

***Abstract*—Network reconfiguration (NR) is a highly complex combinatorial problem with discrete and nonlinear characteristics. With the expansion of the distribution network (DN), solving the NR problem faces the challenge of high dimensions. In this article, we propose a structural decomposition approach (SDA), where the NR problem is suitably allocated to three processes: partition, reconfiguration of equivalent networks, and merging. According to the loop in the original DN, the loop-oriented network partition model is proposed to divide the original DN into multiple equivalent networks, including a loop region and a compressed region. The reconfiguration model is built for the equivalent networks, and the solutions for the loop region and compressed region can be obtained. Then the merging model with the correction method is proposed to merge all reconfiguration solutions of equivalent networks, deal with the inconsistent solutions of different equivalent networks, and obtain the optimal reconfiguration solution of the original DN. Numerical case studies were conducted on the IEEE 33-bus and 119-bus DNs. Compared with other heuristic algorithms for solving NR problem, SDA reduces computation time by 70% while ensuring the optimality of NR strategies. These results demonstrate the effectiveness and exceptional performance of the proposed method.**

***Index Terms*—Distribution network reconfiguration (NR), loop-oriented network partition, merging, parallel implementation, structural decomposition.**

NOMENCLATURE

Abbreviations

DA	Dragonfly algorithm.
DN	Distribution network.
DSO	Distributed system operator.
FTU	Feeder terminal unit.
GA	Genetic algorithm.
HSA	Harmony search algorithm.
IBE	Iterative branch exchange.
MILP	Mixed integer linear programming.
MINLP	Mixed integer nonlinear programming.
NR	Network reconfiguration.
PGA	Parallel genetic algorithm.
PSO	Particle swarm optimization.
SDA	Structural decomposition approach.
SOE	Switch opening and exchange.
SOCP	Second-order cone programming.

Parameters

β', η'	Start and end bus of compressed branch $\beta' \to \eta'$.
β_ξ	Bus in the original DN.
$\boldsymbol{B}_{\boldsymbol{\varphi}}$	Set of sectionalizing switches in loop l_m.
$\boldsymbol{B}'_{\boldsymbol{\varphi}}$	Set of open sectionalizing switches for loop l_m in compressed loop solutions $\boldsymbol{s}_{y,m}, y \neq m$.
b_m, t_m	Sectionalizing switch and tie switch in loop l_m.
d_i	Bus degree for bus *i*.
$\boldsymbol{E}_m$	*m*th equivalent network.
l_m, l'_m	*m*th loop in the original and equivalent network.
M	Number of loops in the DN structure.
N	Number of buses in the DN structure.
$\boldsymbol{N}_{Sub}$	Set of substation buses.
P_{c_max}	Upper limit of transferred power by power line.
P_{c_min}	Lower limit of transferred power by power line.
P_N, Q_N	Active and reactive power of bus *N*.
$R_{i\to j}$, $X_{i\to j}$	Resistance and reactance of branch $i \to j$.
$R'_{i\to j}$ $X'_{i\to j}$	Resistance, reactance of compressed branch $i' \to j'$.
r_m	Loop region of equivalent network $\boldsymbol{E}_m$.
$\boldsymbol{r}_{\text{-}m}$	Compressed region of equivalent network $\boldsymbol{E}_m$.
U_{min}, U_{max}	Lower and upper limit of bus voltage.
Ψ_1, Ψ_2	Number of elements in set $\boldsymbol{B}_{\boldsymbol{\varphi}}$, $\boldsymbol{B}'_{\boldsymbol{\varphi}}$.

Variables

α_{ij}	Binary variable indicating whether bus *j* is the parent of bus *i*.
k_{ij}	State of the switch on branch $i \to j$.
k'_{ij}	State of the switch on compressed branch.
$\boldsymbol{K}_{\boldsymbol{S}}, \boldsymbol{K}'_{\boldsymbol{S}}$	Vectors of k_{ij} and k'_{ij}.
P_{fj}, Q_{fj}	Active, reactive power flowing out of bus *j*.
P'_{fj}, Q'_{fj}	Active, reactive power flowing out of compressed bus.
P_{ij}	Transferred power by branch $i \to j$.
$P_{loss\_1\to N}$	Active power loss of branch $1 \to N$.
$Q_{loss\_j\to(j+1)}$	Reactive power loss of branch $j \to (j+1)$.
$\mathbb{S}$	Solution matrix of all equivalent networks.
$\boldsymbol{S}_{\boldsymbol{E}_m}$	Reconfiguration solution of equivalent network $\boldsymbol{E}_m$.
$s_{m,m}$	Reconfiguration solution of loop region r_m.

Received 3 October 2023; revised 29 June 2024, 13 November 2024, and 23 January 2025; accepted 15 February 2025. Date of publication 15 April 2025; date of current version 13 June 2025. Paper no. TII-23-3606. *(Corresponding author: Nian Liu.)*

Chenchen Li, Nian Liu, Liudong Chen, and Yubing Chen are with the State Key Laboratory of Alternate Electrical Power System with Renewable Energy Sources, North China Electric Power University, Beijing 102206, China (e-mail: cli66@vols.utk.edu; nianliu@ncepu.edu.cn; liudong.c@columbia.edu; chenyubing713@ncepu.edu.cn).

João P. S. Catalão is with the Research Center for Systems and Technologies, Advanced Production and Intelligent Systems Associate Laboratory, Faculty of Engineering, University of Porto, 4200-465 Porto, Portugal (e-mail: catalao@fe.up.pt).

Digital Object Identifier 10.1109/TII.2025.3547040

$\boldsymbol{s}_{m,m-1}$	Reconfiguration solution of compressed loop l'_{m-1}.
$\boldsymbol{S}_{\mathbb{N}}, \boldsymbol{S}'_{\mathbb{N}}$	Feasible solution close to the optimal solution of DN.
U_j	Voltage of bus j.
$\boldsymbol{\Theta}$	Optimal reconfiguration solution of DN.

I. Introduction

With the advancement of electric and electronic technology, the integration of renewable energy sources into distribution networks (DNs) is on the rise. Renewable energy sources bring significant uncertainty [1], [2], [3], [4]. Additionally, the power flow in DN fluctuates with variable nodal power [5]. Consequently, maintaining DN operating in optimal condition with minimum power losses presents a considerable challenge. Network reconfiguration (NR), which optimizes power flow by changing the open/close state of switches, is an effective method for maintaining the DN in optimal condition, especially with the help of high-speed switching devices [6], [7]. However, solving the NR problem is difficult due to its mixed-integer and nonlinear characteristics.

For solving the NR problem, various methods are proposed by researchers. These solving methods can be mainly divided into four categories, as shown in Table I: (1) mathematical optimization techniques, (2) heuristic algorithms, (3) machine learning-based approaches, and (4) parallel computing-based methods. Mathematical optimization techniques reduce the difficulty of solving the NR problem by relaxing the original model. For example, the NR problem is formulated as a second-order cone programming (SOCP) in [8] and as a mixed-integer conic programming in [9]. To consider the impact of NR, active elements, and demand response in a day-ahead scheduling scheme, Vemalaiah et al. [10] build a mixed-integer SOCP and apply Benders decomposition to solve it. Damgacioglu and Celik [11] use a linearized AC power flow model and relax constraints through the second-order cone model. Additionally, the original NR problem can be simplified by relaxing the power flow model into mixed integer linear programming (MILP) [12], [13] and by relaxing the spanning tree constraints through the disjunctive convex hull approach [14]. However, these relaxations may alter the actual values of the power flow, and the calculation time still increases with the scale of the DN.

Various heuristic algorithms are also used to address the NR problem. Harsh and Das [15] propose a two-stage heuristic approach, which includes a sequential switch opening stage and a branch-exchanging stage. A novel iterative branch exchange (IBE) method is proposed to solve the NR problem, combining the traditional branch exchange approach with evolutionary metaheuristic concepts and cluster analysis [16]. Harmony search algorithm (HSA), particle swarm optimization (PSO), switch opening and exchange (SOE) method, dragonfly algorithm (DA), and genetic algorithm (GA) have been applied to obtain the optimal NR strategy [17], [18], [19], [20], [21]. Additionally, a hybrid GA combined with K-nearest neighbors is proposed to solve the NR problem, aiming to minimize power losses, achieve load balancing, and minimize the number of switches [22]. Kim et al. [23] present an encoding and decoding algorithm to simplify the DN and apply GA to solve the NR problem for the simplified DN. However, these heuristic algorithms are time-consuming and can suffer from accuracy loss, as they stochastically generate numerous potential solutions and may overlook the optimal one.

With the popularity of machine learning, several machine learning-based approaches have been developed to solve NR problems. For example, a hybrid data-driven and model-based NR framework is proposed, applying a long short-term memory network to train the mapping mechanism between load distribution and NR strategies [7]. Huang and Zhao [24] integrate the convolutional neural network into the successive branch reduction algorithm for the stochastic NR model, aiming to minimize power losses and enhance voltage stability. Additionally, deep reinforcement learning-based methods are also applied to solve the NR problem. To minimize the cost of power loss and other operation costs, a cloud-edge collaboration framework based on multiagent deep reinforcement learning [25], a two-stage multiagent deep reinforcement learning method [26], and a bigraph neural network modeling-based deep reinforcement learning framework [27] is proposed to solve this problem, respectively. To consider the uncertainty of generation and load in the NR problem, a deep reinforcement learning algorithm with an actor-critic method is developed in [28]. However, machine learning-based approaches depend on extensive databases and involve a time-consuming training process. Deep reinforcement learning-based methods have higher requirements on computation resources and suffer from stability and convergence issues.

These methods discussed earlier are centralized optimization methods. As the scale of the DN expands, centralized optimization methods require more computing resources and longer computation time to solve the NR problem. To address these challenges, the NR problem needs to be developed in a distributed manner. The development of computational resources enables computing tasks to be allocated into many subtasks and implemented in parallel [30]. Parallel computing introduces a new approach to effective NR. For instance, Zhang et al. [29] propose a parallel GA (PGA) to obtain an optimal NR strategy with minimum power losses. However, this approach primarily focuses on the parallel computation of heuristic-solving algorithms by allocating subpopulations across different processors. It does not reduce the inherent complexity of the NR problem.

Indeed, the NR problem is a high-dimensional combinatorial optimization problem characterized by numerous variables and nonlinear, discrete features. Consequently, its complexity will increase exponentially with the expansion of the DN. Additionally, as branches are interconnected and the branch power flow is affected by nodal load, the coupled DN is challenging to be divided into several parts for decentralized solving NR [31]. To address these challenges, this article proposes a structural decomposition approach (SDA), which reduces the dimensionality of the NR problem and supports parallel implementation. The contributions are summarized as follows.

1) An SDA, including loop-oriented network partition, reconfiguration of equivalent networks, and a merging process, is proposed, whose architecture is shown in Fig. 1. It enables the efficient and rapid determination of the optimal NR solution.
2) The loop-oriented network partition model is proposed to decompose the original DN into multiple smaller-scale equivalent networks. Each equivalent network comprises a loop region and a compressed region, with the electrical parameters of the compressed region derived theoretically. The approach transforms a high-dimensional NR problem of the original DN into multiple low-dimensional NR problems in equivalent

TABLE I
SUMMARY OF REFERENCES

Categories	Refs.	Goal	Solving method for NR problem
Mathematical optimization techniques	[8]	Analyze the worthiness of the hourly NR with renewable energy resource, and minimize the power losses	Build a mixed integer SOCP for NR problem, then use MOSEK to solve it
	[9]	Minimize power losses under uncertain generation and load	Build a mixed-integer conic programming for NR problem, then propose a hierarchy method to solve it
	[10]	Minimize the overall cost associated with the operation and management of DN	Build a two-stage stochastic and convex mixed integer SOCP optimization and solve it by Benders decomposition
	[11]	Integrate NR strategy into a multi-period grid operation scheduling problem to minimize the operational costs	Apply linearized AC power flow model, relax constraints by the second order cone model, and use CPLEX to solve NR problem
	[12]	Combine NR problem with conductor selection to minimize power losses and enhance the voltage	Convert original MINLP to the MILP, then use CPLEX to solve this problem
	[13]	Propose a risk-based approach for multi-period NR to minimize power losses cost, power control cost of DG, and customer interruption cost	Build a MILP for NR problem, apply CPLEX to solve it
	[14]	Minimize power losses	Propose disjunctive convex hull approach to relax spanning tree constraints
Heuristic algorithms	[15]	Minimize power losses	A two-stage heuristic approach
	[16]	Minimize power losses and ensure the best voltage level for the transferred load	IBE
	[17]	Minimize power losses	HSA
	[18]	Propose NR model including DG sources, soft open points, and protection devices to minimize power losses	PSO
	[19]	Propose a multi-hour stochastic NR model to minimize energy losses in a period of time	SOE
	[20]	Minimize power losses	DA
	[21]	Optimize scheduling of DG and responsive loads, and conduct hourly reconfiguration	GA
	[22]	Minimize power losses, achieve load balancing, and minimize the number of switching	Hybrid GA combined with K-nearest neighbors
	[23]	Minimize power losses	Present encoding and decoding algorithm to simplify DN, then apply GA to solve NR problem
Machine learning-based approaches	[7]	Minimize power losses	A hybrid data-driven and model-based NR framework
	[24]	Propose a stochastic NR model to minimize power losses and enhance voltage stability	A solving method integrating the convolutional neural network to the successive branch reduction algorithm
	[25]	Minimize the long-term discount power loss cost and the switch operation cost	A cloud-edge collaboration framework based on multi-agent deep reinforcement learning
	[26]	Minimize the cost of photovoltaic power generation curtailment, load shedding, power loss, and switch operations	A two-stage multi-agent deep reinforcement learning method
	[27]	Minimize the cost of power loss, voltage deviation, the switching and tapping costs of all devices	A bi-graph neural network modeling-based deep reinforcement learning framework
	[28]	Minimize the network losses and the cost of switching equipment wear-and-tear, operating the backup generators, and interrupting loads under uncertain generation and load	A deep reinforcement learning algorithm with actor-critic method
Parallel computing-based methods	[29]	Minimize power losses	Parallel GA
	This paper	Minimize power losses	Structural decomposition approach

networks. These low-dimensional NR problems are independent and can be solved in parallel.

3) The merging model with a correction method is proposed to obtain the optimal NR solution of the original DN. Merging all reconfiguration solutions obtained from solving the NR model of equivalent networks can quickly get a feasible solution close to the optimal reconfiguration solution of the original DN. According to the feasible reconfiguration solution, the correction method addresses the potential inconsistency among these reconfiguration solutions of equivalent networks, which guarantees the optimality of the NR solution of the original DN.

II. MATHEMATICAL MODELING

A. Basic Definition

Based on the graph theory, we give the following definitions.

Definition 1 (Bus): In DN, the point at which the load is connected is called a bus, and the ith bus is represented as bus i.

Definition 2 (Branch): The element connecting any two adjacent buses i and j is a branch and is represented as branch $i \to j$. Besides, there is an operable switch on any branch $i \to j$, which is either a sectionalizing switch or a tie switch.

Definition 3 (Loop): A loop l_m is a structure that joins one bus to itself through multiple branches with sectionalizing switches and a branch with a tie switch, e.g., loop l_1, l_2, and l_3 in Fig. 2(a).

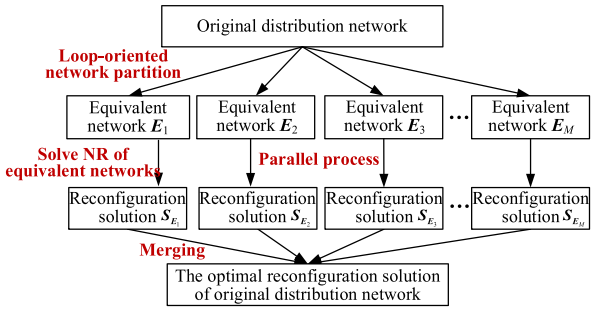

Fig. 1. Architecture of the SDA.

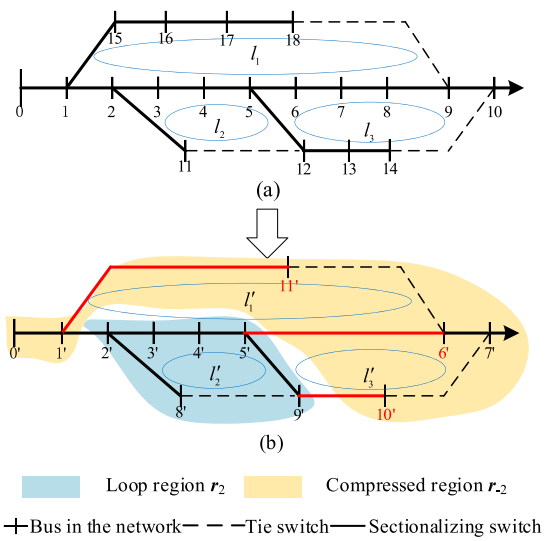

Fig. 2. Structure of DN and equivalent network. (a) Original DN. (b) Equivalent network $\boldsymbol{E}_2$.

The states of all switches can be dynamically changed based on nodal load during the NR process. To operate in a radial structure, one of the switches in a loop should be open.

Definition 4 (DN structure): The DN structure $\mathbb{N}$ is a graph consisting of multiple buses and their associated branches.

Definition 5 (Bus degree): The bus degree d_i for bus i is defined as the number of branches incident on bus i.

Definition 6 (Equivalent network): The equivalent network $\boldsymbol{E}_m$ consists of a loop region r_m and a compressed region $\boldsymbol{r}_{-m}$, which can be represented as follows:

$$\boldsymbol{E}_m \triangleq (r_m, \boldsymbol{r}_{-m}), \ \forall m \in M. \tag{1}$$

Loop l_m in the original DN is the loop region r_m in the equivalent network $\boldsymbol{E}_m$. Excluding loop l_m, all loops $l_y, y \neq m$ with compressed branches form the compressed region $\boldsymbol{r}_{-m}$. Thus, the loop region r_m and the compressed region $\boldsymbol{r}_{-m}$ can be defined as follows:

$$r_m \triangleq l'_m \tag{2}$$

$$\boldsymbol{r}_{-m} \triangleq \left(l'_1, \ldots, l'_{m-1}, \ l'_{m+1}, \ldots, l'_M\right). \tag{3}$$

It is noted there is only one loop l'_m in the loop region r_m, and $l'_m = l_m$. There are M-1 compressed loops in the compressed region $\boldsymbol{r}_{-m}$, which are obtained by compressing the original loops.

Definition 7 (Loop solution): In the equivalent network $\boldsymbol{E}_m$, the reconfiguration solution of the loop region r_m is defined as the loop solution $s_{m,m}$, which is opening a specific switch in the loop region r_m, i.e., a specific switch in the original DN.

Definition 8 (Compressed loop solution): In the equivalent network $\boldsymbol{E}_m$, the reconfiguration solution of the compressed loop $l'_1, \ldots, l'_{m-1}, \ l'_{m+1}, \ldots, l'_M$ is defined as the compressed loop solution $\boldsymbol{s}_{m,1}, \ldots, \boldsymbol{s}_{m,m-1}, \ \boldsymbol{s}_{m,m+1}, \ldots, \boldsymbol{s}_{m,M}$. The compressed loop solution $\boldsymbol{s}_{m,m-1}$ is opening one switch on branches in the compressed loop l'_{m-1}. Since one compressed branch in the compressed loop l'_{m-1} may correspond to several branches in the original DN, the compressed loop solution is a switch set.

Definition 9 (Reconfiguration solution of equivalent network): The reconfiguration solution $\boldsymbol{S}_{E_m}$ of equivalent network $\boldsymbol{E}_m$ consists of a loop solution $s_{m,m}$ and multiple compressed loop solutions $\boldsymbol{s}_{m,1}, \ldots, \boldsymbol{s}_{m,m-1}, \boldsymbol{s}_{m,m+1}, \ldots, \boldsymbol{s}_{m,M}$, i.e., (4).

$$\boldsymbol{S}_{E_m} \triangleq \left(\boldsymbol{s}_{m,1}, \ldots, \boldsymbol{s}_{m,m-1}, s_{m,m}, \boldsymbol{s}_{m,m+1}, \ldots, \boldsymbol{s}_{m,M}\right). \tag{4}$$

Definition 10 (Optimal reconfiguration solution of original DN): The optimal reconfiguration solution Θ of the original DN is the solution with minimum power loss, which is obtained based on multiple reconfiguration solutions of equivalent networks.

One of the equivalent networks of DN is shown in Fig. 2(b). According to Definition 6, the loop region r_2 is the loop l_2, and the compressed region $\boldsymbol{r}_{-2}$ is composed of the compressed loop l'_1 and l'_3. Additionally, the equivalent network's branches in red are compressed branches. The loop solution $s_{2,2}$ in the equivalent network $\boldsymbol{E}_2$ is opening the specific switch on one of the branches 2' $\rightarrow$ 3', 3' $\rightarrow$ 4', 4' $\rightarrow$ 5', 2' $\rightarrow$ 8', 5' $\rightarrow$ 9' or 8' $\rightarrow$ 9' based on Definition 7. Similarly, the compressed loop solution $\boldsymbol{s}_{2,3}$ of the compressed loop l'_3 is opening the switch on one of the branches 5' $\rightarrow$ 6', 6' $\rightarrow$ 7', 5' $\rightarrow$ 9', 9' $\rightarrow$ 10', or 7' $\rightarrow$ 10' based on Definition 8. If the compressed loop solution is opening the switch on compressed branch 5' $\rightarrow$ 6' or 9' $\rightarrow$ 10', the compressed loop solution is a switch set, which includes switch on branches 5 $\rightarrow$ 6, 6 $\rightarrow$ 7, 7 $\rightarrow$ 8, 8 $\rightarrow$ 9, or branches 12 $\rightarrow$ 13, 13 $\rightarrow$ 14, respectively. According to Definition 9, the reconfiguration solution of the equivalent network $\boldsymbol{E}_2$ is $\boldsymbol{S}_{E_2} \triangleq (\boldsymbol{s}_{2,1}, \boldsymbol{s}_{2,2}, \boldsymbol{s}_{2,3})$.

B. NR Problem Formulation

The objective function of the NR problem is minimizing power losses of the DN while satisfying network operational constraints. The reconfiguration model is expressed as follows [17]:

$$\min f \ (\boldsymbol{K}_{\boldsymbol{S}}, U_j) = \sum_{i,j \in r_m} k_{ij} R_{i \to j} \frac{P_{fj}^2 + Q_{fj}^2}{U_j^2} \tag{5}$$

$$s.t. \ P_{c\_min} \leq P_{ij} \leq P_{c\_max} \tag{6}$$

$$U_{\min} \leq U_j \leq U_{\max} \tag{7}$$

$$P_{fj} = P_{f(j+1)} + P_j + P_{loss\_j \to (j+1)} \tag{8}$$

$$Q_{fj} = Q_{f(j+1)} + Q_j + Q_{loss\_j \to (j+1)} \tag{9}$$

$$\sum_{i,j \in N} k_{ij} = N - 1 \tag{10}$$

$$\alpha_{ij} + \alpha_{ji} = k_{ij} \tag{11}$$

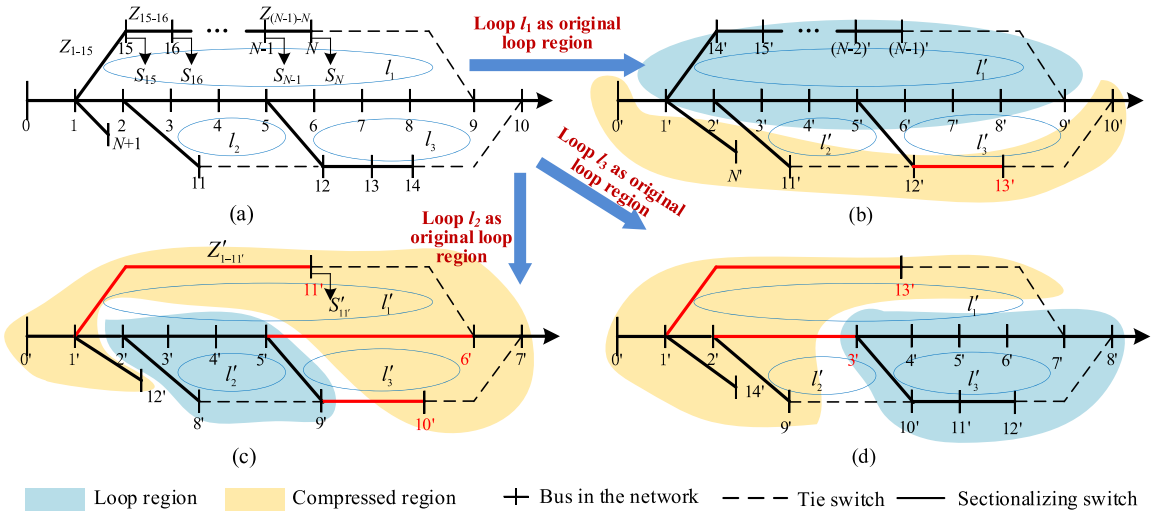

Fig. 3. Loop-oriented network partition process. (a) Original DN. (b) Equivalent network $\boldsymbol{E}_1$. (c) Equivalent network $\boldsymbol{E}_2$. (d) Equivalent network $\boldsymbol{E}_3$.

$$\sum_{j \notin \boldsymbol{N}_{Sub}} \alpha_{ij} = 1 \tag{12}$$

$$\sum_{j \in \boldsymbol{N}_{Sub}} \alpha_{ij} = 0 \tag{13}$$

where (6) and (7) are the constraints of the power line transmission capacity and bus voltage. Equations (8) and (9) show the relationship between the bus power and the power flowing out of the bus. Equations (10)–(13) are the radial structure constraints [32].

III. Structural Decomposition Approach

Solving the NR problem is described as three processes in the proposed SDA: loop-oriented network partition, solving the NR problem of equivalent networks, and merging, as shown in Fig. 1.

A. Loop-Oriented Network Partition

According to the bus degree, all the buses in Fig. 3(a) can be classified into three categories: bus i with degree of 1 ($d_i = 1$), bus j with degree of 2 ($d_j = 2$), and bus r with degree greater than 2 ($d_r > 2$). The bus i ($d_i = 1$) can be regarded as a load of the bus to which it is directly connected (e.g., bus N+1 is regarded as a load of bus 1). Under the scenario with all tie switches open, there are sequentially connected buses with a degree of 2 (e.g., buses 15, 16, …, N-1 in the loop l_1). The load of buses 15, 16, …, N-1, and next bus N can be accumulated on one bus, which is the compressed bus. The compressed branch is also obtained based on the corresponding branches. The bus r ($d_r > 2$) always serves as the end bus of these compressible buses.

Therefore, the loop-oriented network partition model is proposed to solve the problem of loops being coupled in the DN. Its principle is that the equivalent network $\boldsymbol{E}_m$ is obtained by leaving branches in the loop l_m uncompressed (forming loop region l_m) and compressing branches in other loops $l_y, y \neq m$ (forming compressed region $\boldsymbol{r}_{\text{-}m}$). Keep branches in each loop uncompressed separately until getting M equivalent networks of original DN with M loops. Additionally, compress sequentially connected bus i ($d_i = 2$) and the adjacent bus j ($d_j \neq 2$) into one bus, and corresponding switches are compressed to one switch, which can be expressed as (14). Moreover, if branch $i \to j$ is contained in both loop l_m and loop $l_y, y \neq m$, branch $i \to j$ is not compressed. The result of loop-oriented network partition is expressed as (15). The degree of buses $\beta_2, \beta_3, \ldots, \beta_{\xi-1}$ is 2, and the degree of buses β_1 and β_ξ is not 2.

$$\begin{aligned} &\text{branch } \beta' \to \eta' \\ &\triangleq \text{branches } (\beta_1 \to \beta_2,\ \beta_2 \to \beta_3, \ldots,\ \beta_{\xi-1} \to \beta_\xi) \end{aligned} \tag{14}$$

$$\mathbb{N} \triangleq (\boldsymbol{E}_1, \boldsymbol{E}_2, \ldots, \boldsymbol{E}_M)\,. \tag{15}$$

In Fig. 3, 3 equivalent networks are obtained from the original DN based on the loop-oriented network partition model. Taking equivalent network $\boldsymbol{E}_2$ (loop l_2 as the loop region r_2) as an example, buses 6, 7, 8, 9; 15, 16, …, N-1, N; and 13, 14 in Fig. 3(a) are compressed to bus 6', 11', and 10', respectively, in Fig. 3(c). Branches 5' $\to$ 6', 1' $\to$ 11' in loop l_1, and branch 9' $\to$ 10' in loop l_3 are compressed branches after partition, which are the red part in Fig. 3(c). Loops l_1 and l_3 form the compressed region $\boldsymbol{r}_{\text{-}2}$. Note that branches 2 $\to$ 3, 3 $\to$ 4, and 4 $\to$ 5 are in both the compressed region $\boldsymbol{r}_{\text{-}2}$ and the loop region r_2.

To identify the equivalent network with a compressed region $\boldsymbol{r}_{\text{-}m}$, the electrical parameters (i.e., resistance, reactance, reactive power, and active power) should be obtained from the loop-oriented network partition model. Consider the branch 1 $\to N$ in Fig. 3(a) as an example to illustrate the partition model. The resistance and reactance of the equivalence branch 1 $\to$ 11' in Fig. 3(c) should satisfy the following equations:

$$R'_{1\to11'} = R_{1\to15} + R_{15\to16} + \ldots + R_{(N-1)\to N} \tag{16}$$

$$X'_{1\to11'} = X_{1\to15} + X_{15\to16} + \ldots + X_{(N-1)\to N}. \tag{17}$$

For bus 1, the load of buses 15, 16, …, N-1, N should be equivalent to the load of bus 11'. The equivalent load of bus 11' is not a simple sum of the load of buses 15, 16, …, N-1, N, because there is power loss in branches. The power equivalence process aims to provide the same power losses when the power goes through branches 1 $\to N$ and 1 $\to$ 11', whereas the equivalent load of bus 11' is obtained from buses 15, 16, …, N-1, N. Under

the constant bus voltage, the power losses of branches $1 \to N$ and $1 \to 11'$ are calculated as follows [7]:

$$P_{loss\_1\to N} = \frac{(P_{15}+P_{16}+\ldots+P_N)^2}{U_{15}^2} R_{1\to 15} + \frac{(P_{16}+\ldots+P_N)^2}{U_{16}^2} R_{15\to 16} + \ldots + \frac{{P_N}^2}{U_N^2} R_{(N-1)\to N} \tag{18}$$

$$P_{loss\_1\to 11'} = \frac{R'_{1-11'}}{U_{11'}^2} P'^2_{11'}. \tag{19}$$

where $P_{loss\_1\to N}$ and $P_{loss\_1\to 11'}$ are the same in the value, $P'_{11'}$ is the active power of bus 11'.

Note that the calculation of power loss ignores the influence of reactive power and the downstream active power because the reactive power and power loss of a single branch are small. Based on (16), (18), and (19), the calculation method of $P'_{11'}$ is shown as (20) [7]. Similarly, the reactive power $Q'_{11'}$ of bus 11' is calculated by (21) [7]. It can be concluded that the electrical parameters of the compressed branches are determined only by the corresponding original branches' impedance and nodal load. The loop-oriented network partition model remains the compressed region $\boldsymbol{r}_{-m}$ unchanged when the structure of loop region r_m changes, which can avoid dynamic network equivalence and reduce the complexity and time of network equivalence.

$$P'_{11'} = \sqrt{\frac{(P_{15}+P_{16}+\ldots+P_N)^2 R_{1\to 15}}{(R_{1\to 15}+R_{15\to 16}+\ldots+R_{(N-1)\to N})} + \frac{(P_{16}+\ldots+P_N)^2 R_{15\to 16}}{(R_{1\to 15}+R_{15\to 16}+\ldots+R_{(N-1)\to N})} + \ldots + \frac{{P_N}^2 R_{(N-1)\to N}}{(R_{1\to 15}+R_{15\to 16}+\ldots+R_{(N-1)\to N})}} \tag{20}$$

$$Q'_{11'} = \sqrt{\frac{(Q_{15}+Q_{16}+\ldots+Q_N)^2 X_{1\to 15}}{(X_{1\to 15}+X_{15\to 16}+\ldots+X_{(N-1)\to N})} + \frac{(Q_{16}+\ldots+Q_N)^2 X_{15\to 16}}{(X_{1\to 15}+X_{15\to 16}+\ldots+X_{(N-1)\to N})} + \ldots + \frac{{Q_N}^2 X_{(N-1)\to N}}{(X_{1\to 15}+X_{15\to 16}+\ldots+X_{(N-1)\to N})}}. \tag{21}$$

B. Reconfiguration Model of the Equivalent Network

According to the reconfiguration model (5)–(13), the reconfiguration model of the equivalent network $\boldsymbol{E}_m$ obtained by the loop-oriented network partition is expressed as follows:

$$\min f\left(\boldsymbol{K_S}, \boldsymbol{K'_S}, U_j\right) = \sum_{i,j\in r_m} k_{ij} R_{i\to j} \frac{P_{fj}^2 + Q_{fj}^2}{U_j^2} + \sum_{ij\in r_{-m}} k'_{ij} R_{i\to j'} \frac{{P'_{fj}}^2 + {Q'}_{fj}^2}{U_j^2} \tag{22}$$

$$\text{s.t. } (6)\text{–}(13). \tag{23}$$

The reconfiguration solution $\boldsymbol{S}_{E_m}$ of the equivalent network can be obtained by the branch-exchange method. The method can find the loop solution and compressed loop solutions by constantly exchanging the switches' states. Its solving process involves selecting the exchanged switches, calculating the corresponding power loss after exchanging selected switches' states, and determining whether the switches' states should be retained based on the power losses. During the exchange process, two conditions can result in the reduction of DN's power loss [33]: (1) there is a significant voltage difference on the branch with a tie switch, (2) the opened sectionalizing switch is on the lower voltage side of the branch with the tie switch.

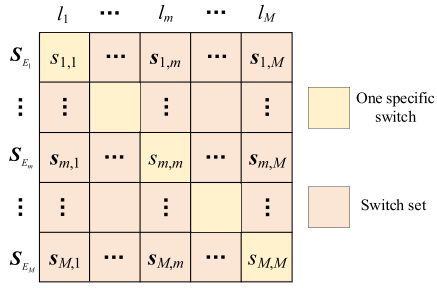

Fig. 4. Composition of reconfiguration solutions of equivalent networks.

C. Merging Model

The reconfiguration solution $\boldsymbol{S}_{E_m}$ of equivalent network $\boldsymbol{E}_m$ is obtained by solving the reconfiguration model. Since each equivalent network contains the information of the original DN and maintains the structure of the original DN, the solution of each equivalent network contains the information of the optimal solution of the original DN. Therefore, merging all reconfiguration solutions $\boldsymbol{S}_{E_m}$ of equivalent networks $\boldsymbol{E}_m$ can quickly get the optimal reconfiguration solution Θ of the original DN.

According to Definitions 7–9, the solution of the equivalent network includes one specific switch and multiple switch sets of original DN. The composition of their reconfiguration solutions is shown in Fig. 4. Each row in Fig. 4 represents the solution of one equivalent network. There are M solutions for the loop l_m in M equivalent networks, i.e., one specific switch (loop solution $s_{m,m}$) and M-1 switch sets (compressed loop solution $\boldsymbol{s}_{m,y},\ y \neq m$). Since the loop l_m is not compressed in the equivalent network $\boldsymbol{E}_m$, the loop solution $s_{m,m}$ is obtained. However, the loop l_m is compressed in the equivalent network $\boldsymbol{E}_y,\ y \neq m$, thus the compressed loop solution $\boldsymbol{s}_{m,y},\ y \neq m$ is obtained. Moreover, the original DN that generates M equivalent networks is the same one and there is only one optimal solution for one loop, thus, solutions of the loop l_m obtained from different equivalent networks should be the same. That is, multiple compressed loop solutions $\boldsymbol{s}_{1,m}, \ldots, \boldsymbol{s}_{m-1,m}, \boldsymbol{s}_{m+1,m}, \ldots, \boldsymbol{s}_{M,m}$ are the same, i.e., (24). Besides, the loop solution $s_{m,m}$ is the subset of the compressed loop solutions $s_{m,y},\ y \neq m$, shown as (25).

$$\boldsymbol{s}_{1,m} = \ldots = \boldsymbol{s}_{m-1,m} = \boldsymbol{s}_{m+1,m} = \ldots = \boldsymbol{s}_{M,m} \tag{24}$$

$$s_{m,m} \subseteq \boldsymbol{s}_{y,m},\ y \neq m. \tag{25}$$

Take equivalent networks in Fig. 3 as examples. If the loop solution $s_{2,2}$ of loop l_2 in equivalent network $\boldsymbol{E}_2$ [Fig. 3(c)] is opening one switch on branches 2' $\to$ 3', 3' $\to$ 4', or 4' $\to$ 5', the compressed loop solution $\boldsymbol{s}_{1,2}$ of loop l_2 in equivalent network $\boldsymbol{E}_1$ [Fig. 3(b)] should be opening the switch on the same branch, the compressed loop solution $\boldsymbol{s}_{3,2}$ of loop l_2 in equivalent network $\boldsymbol{E}_3$ [Fig. 3(d)] should be opening the switch on branch 2' $\to$ 3'. The reason for $\boldsymbol{s}_{1,2} = s_{2,2} \subset \boldsymbol{s}_{3,2}$ is that branches 2 $\to$

3, $3 \rightarrow 4$, and $4 \rightarrow 5$ are not compressed in equivalent network $\boldsymbol{E}_1$ but compressed in equivalent network $\boldsymbol{E}_3$.

However, the method of compressing branches is dependent on the bus degree. If none of the buses in the DN have bus degree greater than 2, the method of compressing branches is fully valid. If one bus degree is greater than 2, the method of compressing branches will result in some deviation in the power losses. The reason is that the power losses of the DN are affected by all branches' impedance and all nodal loads. The little deviation of power losses would result in the inconsistency of solutions for one loop obtained from different equivalent networks. Therefore, a merging model with correction method is proposed to quickly obtain the optimal solution of the original DN. The details of implementation are as follows.

Step 1: Merge NR solutions of equivalent networks

NR solutions of equivalent networks are merged to get a solution matrix and a feasible solution close to the optimal reconfiguration solution Θ of the original DN, which is shown in (26) and (27). The row vector in the solution matrix is the NR solution of the corresponding equivalent network, and the column vector is the solutions for one loop in different equivalent networks.

Step 2: Evaluate consistency of solutions

For one loop l_m, if compressed loop solutions $\boldsymbol{s}_{y,m},\ y \neq m$, and the loop solution $s_{m,m}$ satisfy (24) and (25), the loop solution $s_{m,m}$ might be the optimal solution. It is noted that satisfying (24) and (25) cannot ensure the loop solution is optimal one due to the small deviation caused by the compression. Therefore, the following correction method is needed. If (24) and (25) are not satisfied by compressed loop solutions $\boldsymbol{s}_{y,m},\ y \neq m$ and the loop solution $s_{m,m}$, the corresponding corrections also need to be performed.

$$\mathbb{S} \triangleq \begin{pmatrix} \boldsymbol{S}_{E_1} \\ \vdots \\ \boldsymbol{S}_{E_m} \\ \vdots \\ \boldsymbol{S}_{E_M} \end{pmatrix} \triangleq \begin{pmatrix} s_{1,1} & \cdots & \boldsymbol{s}_{1,m} & \cdots & \boldsymbol{s}_{1,M} \\ \vdots & & \vdots & & \vdots \\ \boldsymbol{s}_{m,1} & \cdots & s_{m,m} & & \boldsymbol{s}_{m,M} \\ \vdots & & \vdots & \cdots & \vdots \\ \boldsymbol{s}_{M,1} & \cdots & \boldsymbol{s}_{M,m} & \cdots & s_{M,M} \end{pmatrix} \tag{26}$$

$$\boldsymbol{S}_{\mathbb{N}} \triangleq (s_{1,1}, \ldots, s_{m,m}, \ldots, s_{M,M}). \tag{27}$$

Step 3: Perform the correction method

1) Preliminary Correction of the Loop Solution: The principle of the preliminary correction is to find an improved solution among feasible ones, which are determined by the NR solution $\boldsymbol{S}_{E_m}$ of the equivalent network. The process for generating feasible solutions based on the NR solution $\boldsymbol{S}_{E_m}$ is illustrated in the following. Each NR solution of the equivalent network is further optimized through this preliminary correction.

The NR solution is the set of open switches in all loops. According to the loop solution and the compressed loop solutions within the NR solution $\boldsymbol{S}_{E_m}$ of the equivalent network, the set of feasible open switches for each loop is identified. All feasible solutions based on the equivalent network $\boldsymbol{E}_m$ are then derived by combining these sets.

a) Determine the feasible open switches for loop l_m: The set of feasible open switches (i.e., $\boldsymbol{Z}_{Sm}$) for loop l_m is determined based on the following equation:

$$\boldsymbol{Z}_{Sm} \triangleq \begin{cases} (\boldsymbol{B}_\varphi, t_m), \varphi \in \Psi_1, & \text{if } flag = 0 \text{ and } s_{m,m} = t_m \\ \boldsymbol{B}'_\varphi, \varphi \in \Psi_2, & \text{if } flag = 0 \text{ and } s_{m,m} \neq t_m \\ (b_{1,m}, t_m), & \text{if } flag = 1 \text{ and } s_{m,m} = t_m \\ (b_{2,m}, t_m), & \text{if } flag = 1 \text{ and } s_{m,m} \neq t_m \end{cases} \tag{28}$$

where the value of *flag* indicates if the loop solution $s_{m,m}$ and compressed loop solutions $\boldsymbol{s}_{y,m},\ y \neq m$ for loop l_m satisfy (24) and (25). If so, *flag* $= 1$, otherwise, *flag* $= 0$. t_m is the tie switch in loop l_m, $s_{m,m} = t_m$ means the loop solution is opening the tie switch, otherwise, opening a sectionalizing switch. $b_{1,m}$ is the sectionalizing switch being on the lower voltage side of the branch with tie switch t_m. $b_{2,m}$ is the open sectionalizing switch in the loop solution $s_{m,m}$.

b) Determine the feasible open switches for loops $l_y, y \neq m$: The set of feasible open switches (i.e., $\boldsymbol{Z}_{Sy}$) for loop l_y, $y \neq m$ is determined based on the following equation:

$$\boldsymbol{Z}_{Sy} \triangleq \begin{cases} (b_{1,y}, t_y), & \text{if } \boldsymbol{s}_{m,y} = t_y \\ (b_{2,y}, t_y), & \text{if } \boldsymbol{s}_{m,y} \neq t_y \end{cases}, \forall y \in M, y \neq m \tag{29}$$

where $\boldsymbol{s}_{m,y} = t_y$ indicates the compressed loop solution is opening the tie switch in loop l_y, otherwise, opening a sectionalizing switch in loop l_y. $b_{1,y}$ is the sectionalizing switch being on the lower voltage side of the branch with tie switch t_y. $b_{2,y}$ is the sectionalizing switch closest to the bus with the lowest voltage among all switches in the compressed loop solution $\boldsymbol{s}_{m,y}$.

The feasible solutions $\boldsymbol{Z}_m$ are obtained by combining these sets of each loop. Then, the solution with the minimum power losses is selected as the improved NR solution, which is closer to the optimal reconfiguration solution Θ than the solution $\boldsymbol{S}_{\mathbb{N}}$. $g(\boldsymbol{Z}_m)$ indicates the vectors of switch states.

$$\boldsymbol{Z}_m \triangleq \{(z_m, z_y) | z_m \in \boldsymbol{Z}_{Sm}, z_y \in \boldsymbol{Z}_{Sy}, y \in M, y \neq m\}, \forall m \in M \tag{30}$$

$$\boldsymbol{S}'_{\mathbb{N}} = arg\min\left(f\left(g(\boldsymbol{Z}_m), U_j{}^*\right)\right). \tag{31}$$

2) Final Correction to Get the Solution for the Original Network: After performing the preliminary correction, M improved solutions $\boldsymbol{S}'_{\mathbb{N}}$ are obtained. Among them, the NR solution $\boldsymbol{Z}_1$ with the smallest power losses is selected. Additionally, the loop solution $s_{m,m}$ is selected from these improved solutions to compose a new NR solution $\boldsymbol{Z}_2$. New feasible solutions $\boldsymbol{Z}'_m$ are obtained by combining $\boldsymbol{Z}_1$ and $\boldsymbol{Z}_2$. Finally, the solution with the minimum power losses is the optimal NR solution for the original network.

$$\boldsymbol{Z}'_m \triangleq \{z_m | z_m \in \boldsymbol{Z}_1 or\ z_m \in \boldsymbol{Z}_2, m \in M\} \tag{32}$$

$$\Theta = arg\min\left(f\left(g\left(\boldsymbol{Z}'_m\right), U_j{}^*\right)\right). \tag{33}$$

D. Overall Solution Process

According to the above mentioned models, the detailed solution process of the proposed SDA is expressed as shown in Algorithm 1.

IV. Case Study

The IEEE 33-bus [34] and 119-bus [35] DN are used to verify the performance of the proposed method.

Algorithm 1: Overall Solution Process.

1. Input the initial electrical parameters R_{i-j}, X_{i-j}, P_j, and Q_j of the DN, the number of switches in loop l_m (n_m), and the number of loops (M).
2. Perform the loop-oriented network partition to obtain multiple equivalent networks $\boldsymbol{E}_m$, and calculate the electrical parameters R'_{i-j}, X'_{i-j}, P'_j and Q'_j of each equivalent network based on (16), (17), (20), and (21).
3. Solve the reconfiguration problem parallelly based on the obtained equivalent networks $\boldsymbol{E}_m$.

For each equivalent network $\boldsymbol{E}_m$:
Calculate the initial power losses $P_{loss,0}$ based on the bus power.
Optimize the equivalent network structure based on the branch-exchange method.
For $m = 1$ to M
Determine the high/low voltage side of the branch with the tie switch, then select the sectionalizing switch to close.
For $h = 1$ to n_m
Open the selected sectionalizing switch in branch h.
If (6)–(13) are true
Calculate the power losses $P_{loss,h}$ based on (22).
If $P_{loss,h} < P_{loss,h-1}$
Close this sectionalizing switch in branch h and select the next sectionalizing switch in the same direction.
Else
Keep the state of the selected switches in the original states.
Break
End If
Else
Break
End If
End For h
End For m

4. According to (26), merge the reconfiguration solutions $\boldsymbol{S}_{\boldsymbol{E}_m}$ of all equivalent networks $\boldsymbol{E}_m$.

Then, evaluate the consistency of solutions.
Next, correct the solution based on (28)–(33).
For each NR solution $\boldsymbol{S}_{\boldsymbol{E}_m}$ of the equivalent network:
Get the feasible open switches set $\boldsymbol{Z}_{Sm}$ for loop l_m based on (28)
Get the feasible open switches set $\boldsymbol{Z}_{Sy}$ for loops l_y, $y \neq m$ based on (29)
Combine $\boldsymbol{Z}_{Sm}$ and $\boldsymbol{Z}_{Sy}$ to get feasible solutions based on (30)
Select the improved NR solution $\boldsymbol{S}'_{\mathbb{N}}$ with the minimum power losses among feasible solutions based on (31)
Until $m = M$, M improved solutions are obtained.
Select the NR solution $\boldsymbol{Z}_1$ with the smallest power losses from these improved solutions
Extract the loop solution from these improved solutions to compose a new NR solution $\boldsymbol{Z}_2$
Combine $\boldsymbol{Z}_1$and $\boldsymbol{Z}_2$ to get new feasible solutions based on (32)
Finally, select the NR solution with the minimum power losses among new feasible solutions based on (33). This solution is the optimal NR solution $\boldsymbol{\Theta}$ of the original DN.

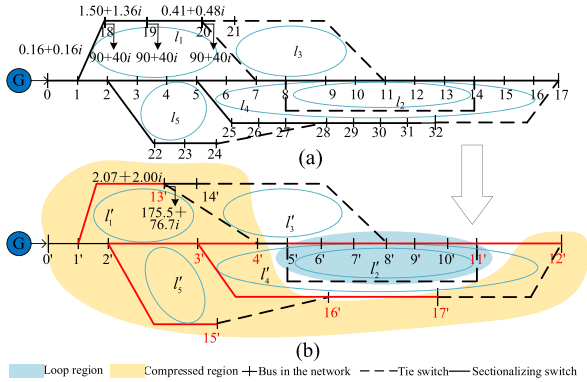

Fig. 5. IEEE 33-bus DN and equivalent network with original loop region l_2. (a) IEEE 33-bus DN. (b) 18-bus network.

TABLE II
RECONFIGURATION SOLUTION OF EQUIVALENT NETWORK

Solution	Loop 1	Loop 2	Loop 3	Loop 4	Loop 5
$\boldsymbol{S}_{E_1}$	7 → 20	8 → 14	8 → 9, 9 → 10, 10 → 11	17 → 32	5 → 25, 25 → 26, 26 → 27, 27 → 28
$\boldsymbol{S}_{E_2}$	7 → 20	8 → 14	9 → 10	17 → 32	5 → 25, 25 → 26, 26 → 27, 27 → 28
$\boldsymbol{S}_{E_3}$	7 → 20	8 → 14	10 → 11	17 → 32	5 → 25, 25 → 26, 26 → 27, 27 → 28
$\boldsymbol{S}_{E_4}$	7 → 20	8 → 14	10 → 11	17 → 32	27 → 28
$\boldsymbol{S}_{E_5}$	7 → 20	8 → 14	8 → 9, 9 → 10, 10 → 11	17 → 32	27 → 28

A. Case I: IEEE 33-Bus DN

1) Results of Loop-Oriented Network Partition: The IEEE 33-bus DN, shown in Fig. 5(a), has 5 loops and 37 branches, which include 32 sectionalizing switches and 5 tie switches. According to the loop-oriented network partition, 5 different equivalent networks are obtained. Fig. 5(b) shows the equivalent network $\boldsymbol{E}_2$ with the loop region r_2. According to the loop-oriented network partition model, branch 5' → 6' belongs to both loop region r_2 and compressed region $\boldsymbol{r}_{-2}$, which should be uncompressed. Comparing Fig. 5(a) and (b), it is clear that branch 1' → 13' is the compressed branch of branches 1 → 18, 18 → 19, 19 → 20, and bus 13' is the compressed bus of buses 18, 19, and 20. In addition, based on (16), (17), (20), and (21), the impedance of branch 1' → 13' is $2.07 + 2.0i$ and the complex power of compressed bus 13' is $175.5 + 76.7i$ kVA. The DN structure is simplified by the loop-oriented network partition, while the information and parameters of buses and branches as well as the network structure are retained in the equivalent network. Therefore, the solution space of the NR problem and computation time of NR solving time are reduced.

2) Results of Reconfiguration and Merging: The reconfiguration solutions of equivalent networks are obtained by parallel performing the branch-exchange processes, which are shown in Table II. The switch set is the compressed loop solution, and only one switch in the switch set is opened to satisfy the radial operation requirement of the DN.

From Table II, it is evident that there is one switch opening in the loop region r_m, i.e., loop solution $s_{m,m}$, and a switch set in the compressed region $\boldsymbol{r}_{-m}$, i.e., compressed loop solution $\boldsymbol{s}_{m,y}$, $y \neq m$. The loop solutions of equivalent networks are

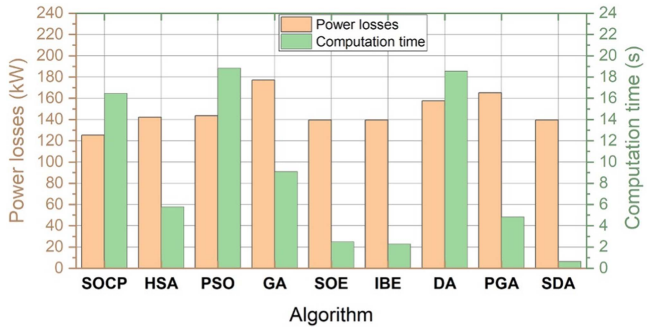

Fig. 6. NR results of the IEEE 33-bus DN obtained by different methods.

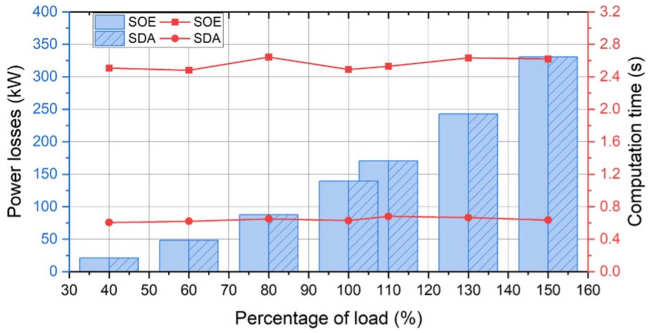

Fig. 7. NR results of the IEEE 33-bus DN under different percentages of load.

on the diagonal of Table II. Take equivalent network $\boldsymbol{E}_5$ as an example. The opened switch on branch 27 → 28 of loop region r_5 is a specific opened switch, but there are multiple switches on the compressed region $\boldsymbol{r}$-$_5$. For loop l_3 of equivalent network $\boldsymbol{E}_3$, the loop solution $s_{3,3}$ is opening the switch on the branch 10 → 11, which is the subset of the compressed loop solution $\boldsymbol{s}_{1,3}$ with opening one switch on one of the branches 8 → 9, 9 → 10, and 10 → 11 of equivalent network $\boldsymbol{E}_1$. For loop l_3 of equivalent network $\boldsymbol{E}_2$, however, branches 8 → 9, 9 → 10, and 10 → 11 are not compressed and the opened switch is on branch 9 → 10, which is not the same as the loop solution $s_{3,3}$. The inconsistency is the result of the small deviation resulting from the loop-oriented network partition. Then, the correction method is performed to correct this inconsistency.

Based on the NR solutions of equivalent networks and the merging model, the optimal reconfiguration solution of the original DN is obtained, which is opening switches on branches 6 → 7, 8 → 9, 13 → 14, 24 → 28, and 31 → 32. The minimum power losses are 139.55 kW, representing a 31% reduction compared to the power losses without optimization (i.e., when all tie switches are open). This reduction occurs because the NR decisions alter the power flow, thereby lowering power losses across these branches. Furthermore, the decreased power losses lead to reduced generation costs.

3) Comparison of the SDA With Different Methods: Fig. 6 shows the comparative results of optimal reconfiguration solutions in terms of the SOCP [8], HSA [17], PSO [18], GA [21], SOE [19], IBE [16], DA [20], PGA [29], and SDA. Note that SDA and PGA are parallel-solving methods, whereas SOCP, HSA PSO, GA, SOE, IBE, and DA are centralized-solving methods. Through performing all these methods in the same computing environment, the same strategies are obtained by the SOCP, SOE, IBE, and SDA. However, the power losses calculated by the SOCP method are smaller compared to those obtained by the SOE, IBE, and SDA. This discrepancy arises because the SOCP method employs convex relaxation, leading to an underestimation of the actual power losses. Therefore, the true minimum power losses are 139.55 kW. Additionally, there are different solutions for HSA, PSO, GA, DA, and PGA because these heuristic algorithms incorporate randomness in their solving processes. As a result, these algorithms may not always converge to a globally optimal solution within their iteration limits.

Regarding the computation time, SOCP, HSA, PSO, GA, SOE, IBE, DA, and PGA are more time-consuming than SDA, which takes 0.63 s (0.15 s for the calculation time of NR and 0.48 s for the merging model). Because solving the NR problem is divided into multiple independent calculation tasks by the loop-oriented network partition, and these tasks are finished in parallel. Additionally, loop-oriented network partitioning is a lightweight computing process. Although the PGA is conducted in parallel, it focuses only on the parallel implementation of the algorithm, ignoring the characteristics of the NR problem.

4) Sensitivity Analysis of the SDA: Considering both peak and off-peak load conditions, a sensitivity analysis of the SDA is conducted based on different load percentages. The 100% load level is referred to as the normal load. Peak load refers to load levels greater than 100%, while off-peak load refers to levels below 100% . To evaluate the robustness of the solution algorithm in terms of optimality, the SOE is also applied to solve the NR problem under these varying load conditions. As shown in Fig. 7, the SDA consistently achieves power losses no greater than those obtained by the SOE across all load conditions. Power losses increase with a higher percentage of load, which is expected due to the increased load flow. Additionally, the computation time of SDA remains nearly constant and is shorter than that of SOE, demonstrating the robustness and efficiency of the proposed SDA.

B. Case II: IEEE 119-Bus DN

1) Reconfiguration Solutions: The proposed SDA is applied to the IEEE 119-bus DN to demonstrate its effectiveness in a large-scale network. The IEEE 119-bus DN contains 15 loops, resulting in 15 different equivalent networks through the loop-oriented network partition model. Then, the reconfiguration models of these equivalent networks are solved in parallel to obtain their NR solutions. Next, merge and correct these NR solutions. Finally, the optimal reconfiguration solution is obtained, i.e., opening switches on branches 44 → 45, 25 → 26, 23 → 24, 45 → 56, 52 → 53, 61 → 62, 41 → 42, 95 → 100, 74 → 75, 77 → 78, 101 → 102, 86 → 113, 89 → 110, 114 → 115, and 35 → 36. Implementing the NR decision can reduce power losses by 34% and significantly lower generation costs compared to the scenario without optimization (i.e., with all tie switches open). This is because the altered power flow from the NR decision decreases power losses across the branches.

2) Comparison of the SDA With Different Methods: The performance of SDA is compared with other existing methods, with the results presented in Fig. 8. Due to the increased number of switches and loops in the IEEE 119-bus DN, the SOCP method struggles to find the optimal solution within an acceptable time range in the current computing environment. This limitation

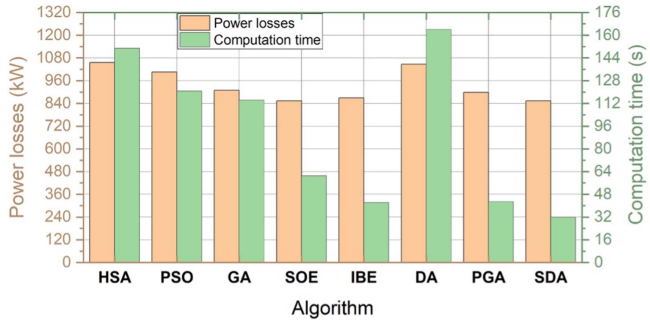

Fig. 8. NR results of the IEEE 119-bus DN obtained by different methods.

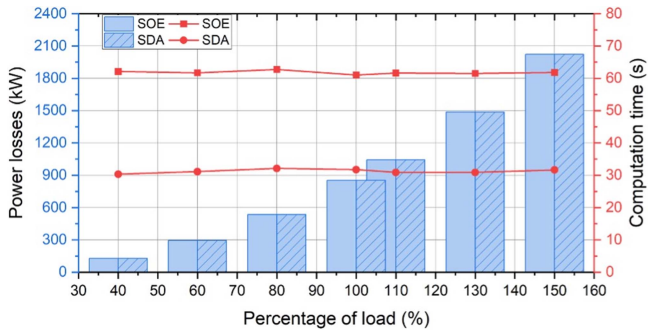

Fig. 9. NR results of the IEEE 119-bus DN under different percentages of load.

indicates the poor scalability of the SOCP method, and therefore, its results are not included in Fig. 8. The minimum power losses (i.e., 853.58 kW) are obtained by the SOE and SDA. Suboptimal solutions with higher power losses are obtained using HSA, PSO, GA, IBE, and DA. Additionally, the computation time of the SDA is the lowest, i.e., 31.76 s, in which the reconfiguration takes 4.12 s and the merging model takes 27.64 s. Other heuristic methods do not reduce the expanding solution space of the NR problem as network size increases, leading to longer computation times. Considering both solution optimality and computation time, the scalability of other methods is inferior to that of the proposed SDA.

3) Sensitivity Analysis of the SDA: Similar to the sensitivity analysis conducted on the IEEE 33-bus DN, a similar study is performed on the IEEE 119-bus DN, with the results shown in Fig. 9. It is evident that the power losses obtained by the SDA are consistently no greater than those from the SOE under different load conditions. Since a larger percentage of load results in increased load flow, power losses also rise with the increase of load. Moreover, the time required by SDA to solve NR problems remains nearly constant across different load conditions and is shorter than that of SOE. Based on this analysis, the SDA proves to be a robust algorithm for solving the NR problem under varying load conditions.

C. Discussions

1) Effectiveness: According to the abovementioned case studies, the proposed SDA obtains the optimal strategy with minimum power losses, ensuring the optimality of the NR problem. For computation time, the SDA reduces computation time by 70% compared to heuristic algorithms such as HSA, PSO, GA, SOE, IBE, DA, and PGA when solving NR problems. The proposed SDA divides the large-scale DN into multiple smaller-scale equivalent networks, reducing the solution space and difficulties. The NR problem of equivalent networks can be solved in parallel. While computation time increases for large-scale networks due to more switches and loops, the SDA still outperforms other methods. Additionally, the computation time can be further reduced with more computing resources available for parallel computing tasks. In conclusion, the proposed SDA is highly effective in solving NR problems.

2) Scalability: The challenges of solving NR problems of large-scale networks are the increased number of loops, variables (switches' actions), and constraints, which prolong computation time and even lead to the failure of some algorithms in identifying the optimal strategy. The proposed SDA addresses this difficulty by dividing the original high-dimensional optimization problem into multiple low-dimensional optimization problems, reducing the complexity of solving NR problems in large-scale networks. These low-dimensional problems can be solved in parallel, further shortening computation time. Additionally, when applying the SDA to solve the NR problem for the IEEE 119-bus DN, we find that the computation time remains at the second-level scale. Successfully and quickly solving the NR problem for the IEEE 119-bus DN demonstrates the scalability of the SDA.

3) Feasibility: In a practical environment, the SDA can be implemented in the existing infrastructure of the smart grid. For example, the distributed system operator (DSO) is generally in charge of the operation of the whole DN, which can implement the NR. With this computation capacity, the loop-oriented network partition model can be performed to obtain many different equivalent networks, and then those equivalent networks can be separated into different cores of their computation resources. Each core can perform the reconfiguration in parallel and then obtain the optimal reconfiguration solution of the original DN through the merging model. If the DSO's computation resources are full, the structure information of the equivalent networks can be broadcasted to each feeder terminal unit (FTU) to perform the reconfiguration with a smaller solution space, and then the merging model can be performed in the DSO. Only several bytes of data are exchanged in the NR process between DSO and FTUs, which can be easily realized. In this study, the SDA is implemented by a computer (e.g., in the DSO) with Intel Core i7-8650U CPU 1.90 GHz, 16 GB memory, and MATLAB 2022a is used as the testing environment. The reconfiguration is parallelly conducted in the different cores of the computer through the *Parfor* function of MATLAB.

4) Robustness: The sensitivity analysis conducted on the IEEE 33-bus and 119-bus DNs demonstrates that the proposed SDA consistently finds the optimal strategy with minimum power losses across varying load conditions. This finding shows the robustness of the proposed SDA in terms of optimality. Furthermore, the variation in computation time required by the SDA to solve the NR problem in different load conditions is small. This further emphasizes its robustness in terms of efficiency. In summary, the proposed SDA exhibits strong robustness in solving NR problems within dynamic environments.

V. Conclusion

In this article, a novel SDA is proposed to achieve parallel NR, in which the NR problem is allocated into three tasks: loop-oriented network partition, solving the NR problem of equivalent networks, and merging. Case studies are conducted on the IEEE 33-bus and 119-bus DNs. Through the loop-oriented network partition model, 5 and 15 equivalent networks are obtained from two DNs, respectively. Their optimal strategies are obtained by solving NR problems of equivalent networks and merging equivalent networks' solutions. Compared to heuristic algorithms such as HSA, PSO, GA, SOE, IBE, DA, and PGA, the SDA reduces computation time by 70% for solving the NR problem while maintaining the optimality of strategies. To sum up, the proposed SDA demonstrates superior performance in solution optimality, computation time, and robustness.

Additionally, quickly obtaining optimal NR strategy can help mitigate issues arising from significant load forecast errors, which cause the DN to deviate from its optimal operational state. However, the effectiveness of the SDA depends on complete information about the DN, including network topology, branch impedance, and nodal power. It is difficult for the SDA to solve the reconfiguration problem of the DN with incomplete information. In future work, we will develop innovative methods to solve the NR problem by incorporating state estimation techniques or machine learning approaches, enabling effective handling of scenarios with incomplete information.

References

[1] F. Khalafian et al., "Capabilities of compressed air energy storage in the economic design of renewable off-grid system to supply electricity and heat costumers and smart charging-based electric vehicles," *J. Energy Storage*, vol. 78, Feb. 2024, Art. no. 109888.

[2] H. Liang and S. Pirouzi, "Energy management system based on economic flexi-reliable operation for the smart distribution network including integrated energy system of hydrogen storage and renewable sources," *Energy*, vol. 293, Apr. 2024, Art. no. 130745.

[3] S. Pirouzi, "Network-constrained unit commitment-based virtual power plant model in the day-ahead market according to energy management strategy," *IET Gener., Transmiss., Distrib.*, vol. 17, pp. 4958–4974, Oct. 2023.

[4] Z. Qu, C. Xu, F. Yang, F. Ling, and S. Pirouzi, "Market clearing price-based energy management of grid-connected renewable energy hubs including flexible sources according to thermal, hydrogen, and compressed air storage systems," *J. Energy Storage*, vol. 69, Oct. 2023, Art. no. 107981.

[5] L. Chen, N. Liu, and J. Wang, "Peer-to-peer energy sharing in distribution networks with multiple sharing regions," *IEEE Trans. Ind. Inform.*, vol. 16, no. 11, pp. 6760–6771, Nov. 2020.

[6] Y. Liu, J. Li, and L. Wu, "Coordinated optimal network reconfiguration and voltage regulator/DER control for unbalanced distribution systems," *IEEE Trans. Smart Grid*, vol. 10, no. 3, pp. 2912–2922, May 2019.

[7] N. Liu, C. Li, L. Chen, and J. Wang, "Hybrid data-driven and model-based distribution network reconfiguration with lossless model reduction," *IEEE Trans. Ind. Inform.*, vol. 18, no. 5, pp. 2943–2954, May 2022.

[8] M. R. Dorostkar-Ghamsari, M. Fotuhi-Firuzabad, M. Lehtonen, and A. Safdarian, "Value of distribution network reconfiguration in presence of renewable energy resources," *IEEE Trans. Power Syst.*, vol. 31, no. 3, pp. 1879–1888, May 2016.

[9] R. A. Jabr, "Mixed integer optimization of the flow pattern for stochastic feeder reconfiguration," *IEEE Trans. Power Syst.*, vol. 39, no. 1, pp. 1896–1904, Jan. 2024.

[10] K. Vemalaiah, D. K. Khatod, and N. P. Padhy, "Synergistic day-ahead scheduling framework for smart distribution grid under uncertainty," *IEEE Trans. Ind. Inform.*, vol. 20, no. 7, pp. 9681–9691, Jul. 2024.

[11] H. Damgacioglu and N. Celik, "A two-stage decomposition method for integrated optimization of islanded AC grid operation scheduling and network reconfiguration," *Int. J. Elect. Power Energy Syst.*, vol. 136, Mar. 2022, Art. no. 107647.

[12] G. Pareja, A. Luis, J. M. López-Lezama, and O. G. Carmona, "Optimal integration of distribution network reconfiguration and conductor selection in power distribution systems via MILP," *Energies*, vol. 16, no. 19, Oct. 2023, Art. no. 6998.

[13] Z. N. Popovic and S. D. Knezevic, "Dynamic reconfiguration of distribution networks considering hosting capacity: A risk-based approach," *IEEE Trans. Power Syst.*, vol. 38, no. 4, pp. 3440–3450, Jul. 2023.

[14] C. Lei, S. Bu, J. Zhong, Q. Chen, and Q. Wang, "Distribution network reconfiguration: A disjunctive convex Hull approach," *IEEE Trans. Power Syst.*, vol. 38, no. 6, pp. 5926–5929, Nov. 2023.

[15] P. Harsh and D. Das, "A simple and fast heuristic approach for the reconfiguration of radial distribution networks," *IEEE Trans. Power Syst.*, vol. 38, no. 3, pp. 2939–2942, May 2023.

[16] E. C. Pereira, C. H. N. R. Barbosa, and J. A. Vasconcelos, "Distribution network reconfiguration using iterative branch exchange and clustering technique," *Energies*, vol. 16, no. 5, 2023, Art. no. 2395.

[17] R. Srinivasa Rao, S. V. L. Narasimham, M. Ramalinga Raju, and A. Srinivasa Rao, "Optimal network reconfiguration of large-scale distribution system using harmony search algorithm," *IEEE Trans. Power Syst.*, vol. 26, no. 3, pp. 1080–1088, Aug. 2011.

[18] A. Azizi, B. Vahidi, and A. F. Nematollahi, "Reconfiguration of active distribution networks equipped with soft open points considering protection constraints," *J. Modern Power Syst. Clean Energy*, vol. 11, no. 1, pp. 212–222, Jan. 2023.

[19] J. Zhan, W. Liu, C. Y. Chung, and J. Yang, "Switch opening and exchange method for stochastic distribution network reconfiguration," *IEEE Trans. Smart Grid*, vol. 11, no. 4, pp. 2995–3007, Jul. 2020.

[20] K. Rahmati and S. Taherinasab, "The importance of reconfiguration of the distribution network to achieve minimization of energy losses using the dragonfly algorithm," *e-Prime - Adv. Elect. Eng., Electron., Energy*, vol. 5, 2023, Art. no. 100270.

[21] S. Golshannavaz, S. Afsharnia, and F. Aminifar, "Smart distribution grid: Optimal day-ahead scheduling with reconfigurable topology," *IEEE Trans. Smart Grid*, vol. 5, no. 5, pp. 2402–2411, Sep. 2014.

[22] S. Jo et al., "Hybrid genetic algorithm with k-nearest neighbors for radial distribution network reconfiguration," *IEEE Trans. Smart Grid*, vol. 15, no. 3, pp. 2614–2624, May 2024.

[23] H.-W. Kim, S.-J. Ahn, S.-Y. Yun, and J.-H. Choi, "Loop-based encoding and decoding algorithms for distribution network reconfiguration," *IEEE Trans. Power Del.*, vol. 38, no. 4, pp. 2573–2584, Aug. 2023.

[24] W. Huang and C. Zhao, "Deep-learning-aided voltage-stability-enhancing stochastic distribution network reconfiguration," *IEEE Trans. Power Syst.*, vol. 39, no. 2, pp. 2827–2836, Mar. 2024.

[25] H. Gao, R. Wang, S. He, L. Wang, J. Liu, and Z. Chen, "A cloud-edge collaboration solution for distribution network reconfiguration using multi-agent deep reinforcement learning," *IEEE Trans. Power Syst.*, vol. 39, no. 2, pp. 3867–3879, Mar. 2024.

[26] H. Gao, S. Jiang, Z. Li, R. Wang, Y. Liu, and J. Liu, "A two-stage multi-agent deep reinforcement learning method for urban distribution network reconfiguration considering switch contribution," *IEEE Trans. Power Syst.*, vol. 39, no. 6, pp. 7064–7076, Nov. 2024.

[27] R. Wang, X. Bi, and S. Bu, "Real-time coordination of dynamic network reconfiguration and volt-VAR control in active distribution network: A graph-aware deep reinforcement learning approach," *IEEE Trans. Smart Grid*, vol. 15, no. 3, pp. 3288–3302, May 2024.

[28] S. Bahrami, Y. C. Chen, and V. W. S. Wong, "Dynamic distribution network reconfiguration with generation and load uncertainty," *IEEE Trans. Smart Grid*, vol. 15, no. 6, pp. 5472–5484, Nov. 2024.

[29] J. Zhang, X. Yuan, and Y. Yuan, "A novel genetic algorithm based on all spanning trees of undirected graph for distribution network reconfiguration," *J. Modern Power Syst. Clean Energy*, vol. 2, no. 2, pp. 143–149, Jun. 2014.

[30] C. H. Liang, C. Y. Chung, K. P. Wong, and X. Z. Duan, "Parallel optimal reactive power flow based on cooperative co-evolutionary differential evolution and power system decomposition," *IEEE Trans. Power Syst.*, vol. 22, no. 1, pp. 249–257, Feb. 2007.

[31] M. Doostmohammadian, H. R. Rabiee, H. Zarrabi, and U. Khan, "Observational equivalence in system estimation: Contractions in complex networks," *IEEE Trans. Netw. Sci. Eng.*, vol. 5, no. 3, pp. 212–224, Jul.–Sep. 2018.

[32] R. A. Jabr, R. Singh, and B. C. Pal, "Minimum loss network reconfiguration using mixed-integer convex programming," *IEEE Trans. Power Syst.*, vol. 27, no. 2, pp. 1106–1115, May 2012.

[33] C. Ababei and R. Kavasseri, "Efficient network reconfiguration using minimum cost maximum flow-based branch exchanges and random walks-based loss estimations," *IEEE Trans. Power Syst.*, vol. 26, no. 1, pp. 30–37, Feb. 2011.

[34] M. E. Baran and F. F. Wu, "Network reconfiguration in distribution systems for loss reduction and load balancing," *IEEE Trans. Power Del.*, vol. 4, no. 2, pp. 1401–1407, Apr. 1989.

[35] D. Zhang, Z. Fu, and L. Zhang, "An improved TS algorithm for loss-minimum reconfiguration in large-scale distribution systems," *Electric Power Syst. Res.*, vol. 77, no. 5, pp. 685–694, Apr. 2007.

Chenchen Li (Graduate Student Member, IEEE) received the B.S. and M.S. degrees in electrical engineering from North China Electric Power University, Beijing, China, in 2019 and 2022, respectively. She is currently working toward the Ph.D. degree in electrical engineering with the University of Tennessee, Knoxville, TN, USA.

Her research interests include distribution system optimization and distribution system planning.

Nian Liu (Member, IEEE) received the B.S. and M.S. degrees in electric engineering from Xiangtan University, Xiangtan, China, in 2003 and 2006, respectively, and the Ph.D. degree in electrical engineering from North China Electric Power University, Beijing, China, in 2009.

He is currently a Professor and also the Vice Dean with the School of Electrical and Electronic Engineering, North China Electric Power University. He is the Director of the Research Section for Multi-information Fusion and Integrated Energy System Optimization, State Key Laboratory of Alternate Electrical Power System, Renewable Energy Sources. From 2015 to 2016, he was a Visiting Research Fellow with the Royal Melbourne Institute of Technology University, Melbourne, Australia. He has authored or coauthored more than 180 journal and conference publications and has been granted more than 20 patents in China. His major research interests include multienergy system integration, microgrids, cyber-physical energy system, and renewable energy integration.

Dr. Liu is an Editor for the IEEE TRANSACTIONS ON SMART GRID, IEEE TRANSACTIONS ON SUSTAINABLE ENERGY, IEEE POWER ENGINEERING LETTERS, and *Journal of Modern Power Systems and Clean Energy* (MPCE). He was a Highly Cited Chinese Researcher of Elsevier from 2020 to 2023.

Liudong Chen (Graduate Student Member, IEEE) received the B.S. and M.S. degrees in electrical engineering from North China Electric Power University, Beijing, China, in 2019 and 2022, respectively. He is currently working toward the Ph.D. degree in earth and environmental engineering with Columbia University, New York, NY, USA.

His research focuses on analyzing and coordinating distributed energy resources through optimization, economics, and machine learning, addressing the challenges related to increasing uncertainty, behavior interdependence, and market adaptation.

Mr. Chen was the recipient of the IEEE Power & Energy Society Outstanding Student Scholarship in 2022.

Yubing Chen is currently working toward the Ph.D. degree in electrical engineering with the North China Electric Power University, Beijing, China.

Her research interests include energy management, power system dispatching, especially energy storage system dispatching.

João P. S. Catalão (Fellow, IEEE) is currently a Full Professor (Professor Catedrático) with the Faculty of Engineering, University of Porto, Porto, Portugal. From 2012 to 2015, he was the Primary Coordinator of the 5.2-million-euro FP7-EU project SiNGULAR. Since 2024, he has been the Primary Coordinator of the 4.5-million-euro Horizon-EU project EU-DREAM. He has coauthored more than 500 journal publications, with an h-index of 105 and more than 40 000 citations (according to Google Scholar), having supervised more than 140 researchers (postdocs, Ph.D. and M.Sc. students, and other students with project grants). His research interests include power system operations and planning, power system economics and electricity markets, distributed renewable generation, demand response, smart grid, and multienergy carriers.

He was the General Chair of SEST 2019 (technically cosponsored by IEEE), after being the inaugural Technical Chair and cofounder of SEST 2018. He was the Editor of two CRC Press Books: *Electric Power Systems: Advanced Forecasting Techniques and Optimal Generation Scheduling* (2012) and *Smart and Sustainable Power Systems: Operations, Planning and Economics of Insular Electricity Grids* (2015). He is a Senior Editor for the IEEE TRANSACTIONS ON NEURAL NETWORKS AND LEARNING SYSTEMS, IEEE TRANSACTIONS ON SYSTEMS, MAN, AND CYBERNETICS: SYSTEMS, and a Senior Associate Editor for the IEEE TRANSACTIONS ON CIRCUITS AND SYSTEMS PART II: EXPRESS BRIEFS. He was an IEEE CIS Fellows Committee Member in 2022–2024 (three consecutive years). He was elected a Full Member of Sigma Xi, The Scientific Research Honor Society, in 2023. He was recognized as an Outstanding Associate Editor 2023 for the IEEE TRANSACTIONS ON EMERGING TOPICS IN COMPUTATIONAL INTELLIGENCE, an Outstanding Associate Editor 2021 for the IEEE TRANSACTIONS ON POWER SYSTEMS, and an Outstanding Senior Associate Editor 2020 for the IEEE TRANSACTIONS ON SMART GRID. Furthermore, he has won five Best Paper Awards at IEEE Conferences. He is among the Top 2% of Scientists, since 2019, and a Best Scientist 2022–2024 in Research.com. He was a Highly Cited Researcher in the field of Engineering in 2023.